ARMY RESEARCH LABORATORY

Distributed Mobile Device Based Shooter Detection Simulation

by David Doria and Peter Schwartz

ARL-TR-6671 September 2013

NOTICES

Disclaimers

The findings in this report are not to be construed as an official Department of the Army position unless so designated by other authorized documents.

Citation of manufacturer's or trade names does not constitute an official endorsement or approval of the use thereof.

Destroy this report when it is no longer needed. Do not return it to the originator.

Army Research Laboratory

Aberdeen Proving Ground, MD 21005-5066

ARL-TR-6671 **September 2013**

Distributed Mobile Device Based Shooter Detection Simulation

David Doria and Peter Schwartz

Computational and Information Sciences Directorate, ARL

REPORT DOCUMENTATION PAGE	Form Approved OMB No. 0704-0188

1. REPORT DATE *(DD-MM-YYYY)*	2. REPORT TYPE	3. DATES COVERED (From - To)
September 2013	Final	08/2013

4. TITLE AND SUBTITLE	5a. CONTRACT NUMBER
Distributed Mobile Device Based Shooter Detection Simulation	5b. GRANT NUMBER
	5c. PROGRAM ELEMENT NUMBER

6. AUTHOR(S)	5d. PROJECT NUMBER
David Doria and Peter Schwartz	R.0006163.13
	5e. TASK NUMBER
	5f. WORK UNIT NUMBER

7. PERFORMING ORGANIZATION NAME(S) AND ADDRESS(ES)	8. PERFORMING ORGANIZATION REPORT NUMBER
U.S. Army Research Laboratory ATTN: RDRL-CIH-S Aberdeen Proving Ground, MD 21005-5066	ARL-TR-6671

9. SPONSORING/MONITORING AGENCY NAME(S) AND ADDRESS(ES)	10. SPONSOR/MONITOR'S ACRONYM(S)
	11. SPONSOR/MONITOR'S REPORT NUMBER(S)

12. DISTRIBUTION/AVAILABILITY STATEMENT

Approved for public release; distribution is unlimited.

13. SUPPLEMENTARY NOTES

14. ABSTRACT

In this report we develop a system for simulating shooter detection under varying system parameters and configurations. First, we discuss the mathematical details of the shooter detection problem. Next, we detail the simulation software that we developed to enable these analyses. We go on to study the performance of the system under various forms of error, including microphone localization error, inter-microphone clock synchronization error, and microphone count and configuration. Analysis is performed to determine, for many different configurations of these system variables, the ability to locate the shooter, as well as the accuracy of the computed location. Finally, we summarize the findings and make recommendations for future system design.

15. SUBJECT TERMS

Shooter detection, Gunshot detection

16. SECURITY CLASSIFICATION OF:			17. LIMITATION OF ABSTRACT	18. NUMBER OF PAGES	19a. NAME OF RESPONSIBLE PERSON
a. REPORT	b. ABSTRACT	c. THIS PAGE			David Doria
Unclassified	Unclassified	Unclassified	UU	44	19b. TELEPHONE NUMBER (*Include area code*) 410-278-2310

Standard Form 298 (Rev. 8/98)
Prescribed by ANSI Std. Z39.18

Contents

List of Figures

1. Introduction

Shooter detection (or gunshot localization) is the problem of determining the location of the source of a gunshot. The ability to do this is very beneficial to the Warfighter. Understanding where a threat is located on the battlefield allows the Warfighter to react appropriately, either by taking cover or returning fire. In a typical situation, multiple Warfighters will hear a gunshot and wish to determine its origin. A sketch of the situation in a shooter detection problem is shown in figure 1.

Figure 1. A sketch of the situation in a shooter detection problem. Multiple observers hear the sound of a gunshot and would like to know where it originated.

In section 1.1, we discuss current commercial and academic systems for gunshot localization. In section 2, we detail two geometric solutions to the problem. These solutions are not novel, but we did not find detailed treatment in the literature, so the details of the solutions are presented here. In section 3, we detail the software that was developed to enable the analyses in this report. In section 4, we present and discuss several experiments that analyze the quality of the gunshot localization under varying system conditions. Finally, in section 5, we draw conclusions from our experiments and make recommendations to aid in the design of future gunshot localization systems.

1.1 Current Systems

Several commercial systems have been developed to solve the shooter detection problem using complex and expensive hardware. Such systems include Boomerang (*1*) and Early Attack Reaction Sensor (EARS) (*2*). Each of these systems requires complex and expensive hardware to achieve its goal.

Academic work (*3*) has shown that a system based on commercial mobile devices with additional hardware modules (external sensors) is feasible. However, it would be ideal from an Army perspective to produce a shooter detection system using only a small network of commercially available, "off-the-shelf" mobile devices (smartphones, tablets, etc.). Keeping the size, weight, and power requirement (SWaP) of a Warfighter's supplies to a minimum is a critical design parameter. In this report, we develop a software tool that could be used to aid in the development of such a system.

2. Determining the Shooter Location

While there are three signatures of a gunshot (muzzle flash [optical], muzzle blast [auditory], and shock wave [auditory]), we focus only on information from the muzzle blast. This decision was made for several reasons. Detecting the muzzle blast does not require any particular proximity to the trajectory of the bullet, while this proximity is important when using information from the shock wave. Detecting and using the muzzle flash would require accurate device orientation information, as well as require the camera to remain active indefinitely, significantly reducing the battery life of the device. Additionally, the mobile device would need to be aimed towards the blast to even have a chance detect the muzzle flash.

2.1 Single Microphone

When a sound is heard by a single, omnidirectional microphone, it is impossible to tell from which direction the sound came, or how far away it originated. That is, the shooter could be anywhere. This situation is shown in figure 2.

2.2 Multiple Microphones

When several microphones are present (e.g., each present on the device of a different Warfighter), we are often able to estimate the location of the gunshot. To simplify the problem, we make

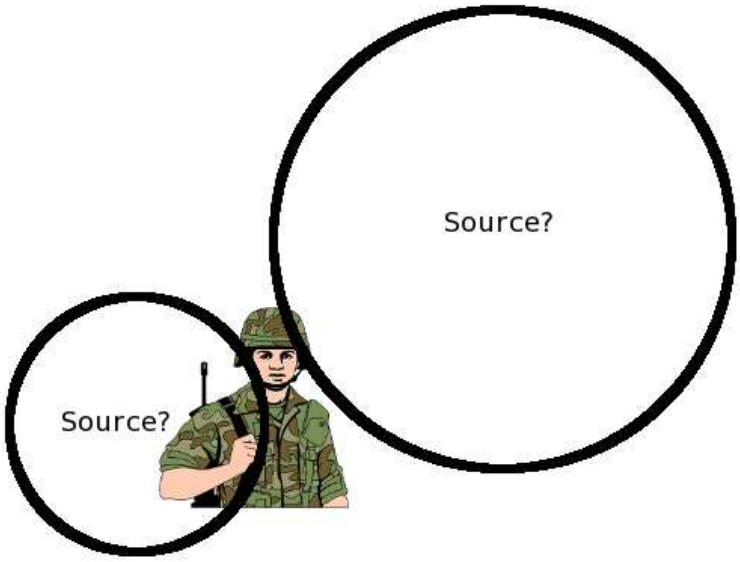

Figure 2. With only one omnidirectional microphone, it is not possible to determine the distance or direction of the origin of a sound. The black circles indicate the spherical propagation of the sound from two possible sources where they intersect the microphone position.

several assumptions. First, we assume that the observers have a direct line of sight to the shooter. That is, there are no occluding objects (building, trees, vehicles, etc.) between the observer positions and the shooter position. Second, we assume that the curvature of the Earth is negligible (a safe assumption at ballistic threat ranges). Third, we assume that the air temperature is constant over both time and position (during each gunshot event) so that the sound of the gunshot travels at a constant speed. Fourth, we assume that the precise moment of the gunshot is able to be determined through signal processing techniques (such as cross-correlation, etc.). Finally, we treat the situation as a two-directional (2-D) problem—that is, we assume the shooter is on the same plane as all of the observers. This assumption is the most easily relaxed, but is left to future work.

There are two ways to approach the geometry of the problem of determining the shooter location, the Hyperbolic Lines of Position (HLOP) method and the Location on the Conic Axis (LOCA) method. In the HLOP method, each microphone is interpreted as the focus of a hyperbola, and the shooter is found to be at the intersection of several such hyperbolas. We studied the HLOP technique extensively (*4*), but determined that the LOCA method is more accurate, applicable in more cases, and easier to implement, so we restrict our attention in this report to analysis of the LOCA method.

2.3 Location On The Conic Axis (LOCA) Method

In the LOCA method, we treat the problem as the mathematical dual of the HLOP method. That is, we treat the microphones as lying on conics and compute the shooter position as a focus of these conics. If we have three microphones, the location of the shooter is known to be at one of the foci of the conic through the microphone locations. However, it is impossible to tell which of the foci is the correct position. Fortunately, with four or more microphones (with all subsets of three microphones not colinear), we can resolve this ambiguity. Interestingly, it is actually not necessary to compute the equations of the conics on which subsets of the microphones lie. Instead, we can determine the location of the shooter by computing the major axes of two or more triads of microphones and finding their intersection.

2.3.1 Determining the Major Axis of a Conic Through Three Points

While five points are required to fully define a conic, it is shown (*5*) that the focus of a conic can be constrained to a line (the major axis) by only three points. This line is given by $Ax + By + C = 0$, where

$$A = x_1 r_{23} + x_2 r_{31} + x_3 r_{12} \tag{1}$$

$$B = y_1 r_{23} + y_2 r_{31} + y_3 r_{12} \tag{2}$$

$$C = -\frac{1}{2}\left(r_{12} r_{23} r_{31} + (x_1^2 + y_1^2) r_{23} + (x_2^2 + y_2^2)^2 r_{31} + (x_3^2 + y_3^2)^2 r_{12}\right) \tag{3}$$

where (x_i, y_i) is the position of the i^{th} microphone and $r_{ij} = r_j - r_i$. A graphical representation of the situation is shown in figure 3.

2.3.2 Determining the Shooter Location as the Intersection of Major Axes of Conics

When we have more than three microphones, we can form multiple conics. As shown in figure 4, the intersection of the major axes of these conics is necessarily the position of the shooter.

From the major axes computed, we can form the linear system

$$\begin{pmatrix} A_1 & B_1 \\ A_2 & B_2 \\ \vdots & \vdots \\ A_{N_T} & B_{N_T} \end{pmatrix} \begin{pmatrix} x \\ y \end{pmatrix} = \begin{pmatrix} -C_1 \\ -C_2 \\ \vdots \\ -C_{N_T} \end{pmatrix} \tag{4}$$

where A_i, B_i, and C_i are the coefficients of the equation of the major axis of the i^{th} triad, and N_T

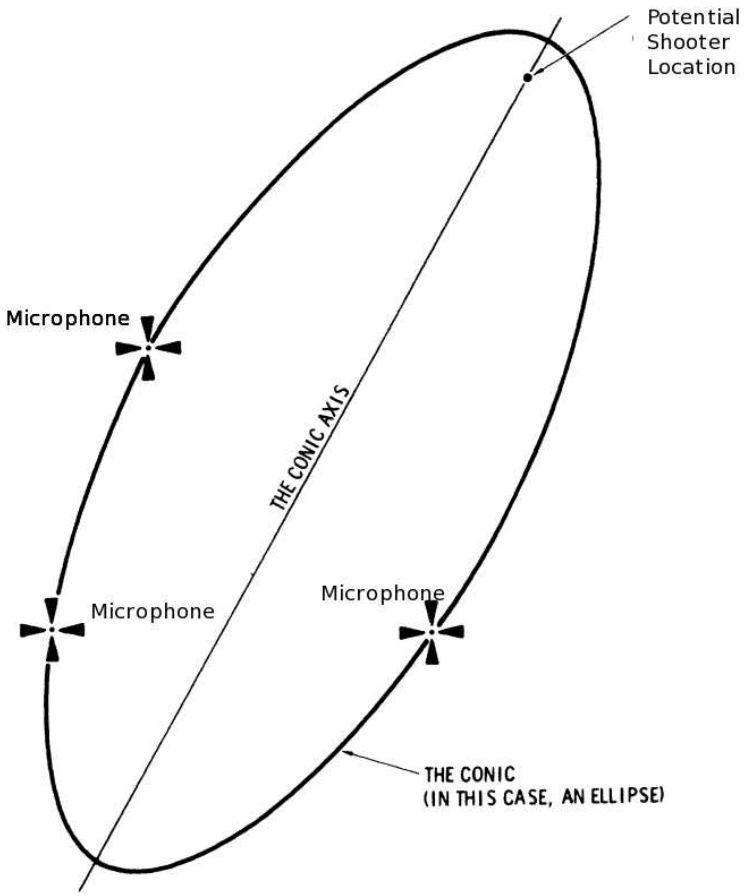

Figure 3. With three microphones, the location of the shooter can be narrowed down to a line—the major axis of an ellipse. (Figure adapted from reference 5).

is the number of triads. If we consider two triads from a set of four microphones, we produce two major axis lines, which (unless there are parallel because of a degenerate configuration) intersect at one point. This point is the location of the shooter. We note that there are $\binom{N_m}{3}$ different triads that can be selected from N_m microphones. As previously mentioned, with three microphones, we only have $\binom{3}{3} = 1$ lines, so we cannot perform the intersection of two lines because there is only one line. With $N_m = 4$ microphones, we have $\binom{4}{3} = 4$ triads, leading to $\binom{4}{2} = 6$ intersections. However, all pairs of two of these triads have major axes that intersect at exactly the same point. While there is no obvious analytical way to prove this, using symbolic

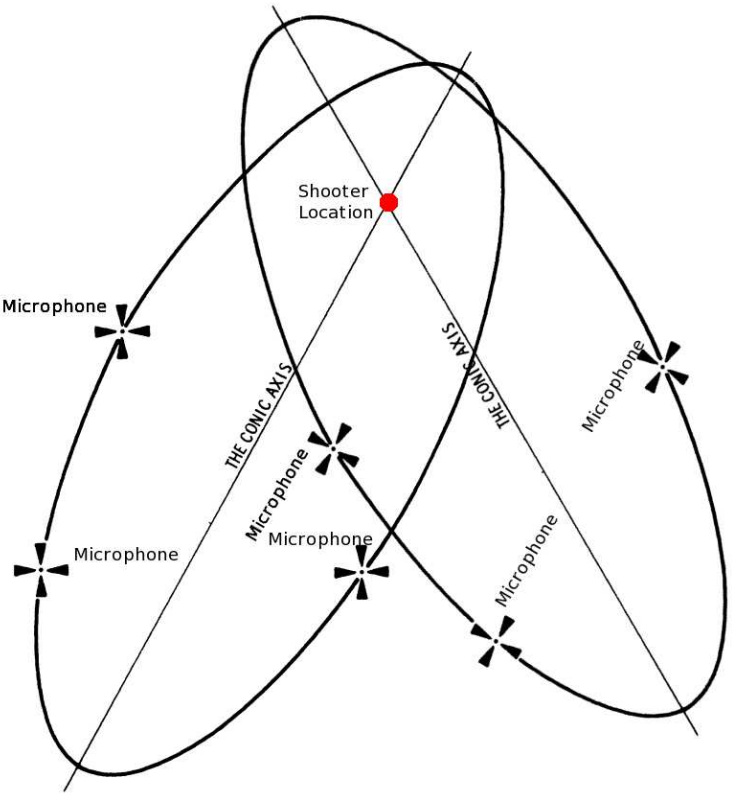

Figure 4. With more than three microphones, the location of the shooter can be computed exactly. (Figure adapted from reference 5).

manipulation software (see the appendix) we can show that

$$\det \begin{pmatrix} A_1 & B_1 & C_1 \\ A_2 & B_2 & C_2 \\ A_3 & B_3 & C_3 \end{pmatrix} = 0 \tag{5}$$

which means that any third major axis is linearly dependent on any other two major axes.

When more than four microphones are available, there are more than two independent major axis lines. The solution is then computed to be the point that best approximates (in a least squares sense) the $\binom{N_m}{4}$ different intersections given by each set of four microphones. If we solve this linear system in equation 4, we would obtain a weighted least squares solution, meaning points with larger coordinate values would incorrectly contribute more to the solution. To compute the desired unweighted solution (minimize the perpendicular distance from the solution to all of the major axis lines), we must first normalize by dividing A_i, B_i, and C_i each by $\sqrt{A_i^2 + B_i^2}$ (as

shown in reference 6) and solve the system

$$\begin{pmatrix} \frac{A_1}{\sqrt{A_1^2+B_1^2}} & \frac{B_1}{\sqrt{A_1^2+B_1^2}} \\ \frac{A_2}{\sqrt{A_2^2+B_2^2}} & \frac{B_2}{\sqrt{A_2^2+B_2^2}} \\ \vdots & \vdots \\ \frac{A_{N_T}}{\sqrt{A_{N_T}^2+B_{N_T}^2}} & \frac{B_{N_T}}{\sqrt{A_{N_T}^2+B_{N_T}^2}} \end{pmatrix} \begin{pmatrix} x \\ y \end{pmatrix} = \begin{pmatrix} -\frac{C_1}{\sqrt{A_1^2+B_1^2}} \\ -\frac{C_2}{\sqrt{A_2^2+B_2^2}} \\ \vdots \\ -\frac{C_{N_T}}{\sqrt{A_{N_T}^2+B_{N_T}^2}} \end{pmatrix}. \tag{6}$$

3. Software Implementation

We have developed a gunshot simulation software suite that allows the user to interactively place any number of microphones, as well as a shooter, in a scene. The main graphical user interface (GUI) window is shown in figure 5. The microphones (presumably carried by Warfighters) are represented by the triple chevrons (the insignia of a sergeant), and the shooter is represented by a gun. By default, four microphones are positioned randomly on the map. Currently, the background image is simply aesthetic and does not affect the simulation. However, a reasonable extension would be to scale the image such that positions overlayed on the image are meaningful relative to the size of the objects in the image.

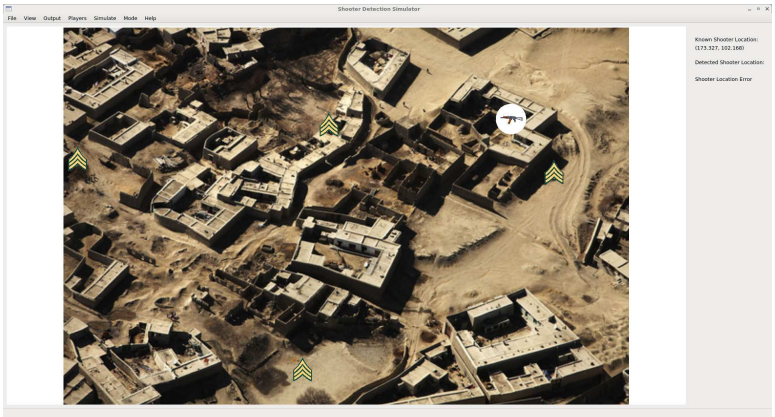

Figure 5. The main GUI of our simulator. The microphones are represented by the sergeant insignia, and the shooter is represented by a gun.

3.1 Gunshot Reception Model

In the simulation, our first goal is to compute the relative receive times of the gunshot sound heard by each microphone. In the most simple case, the receive time at the i^{th} microphone, t_{ri}, is computed as the distance between the known shooter location and the i^{th} microphone, d_i, divided by the speed of the sound, v_s. That is,

$$t_{ri} = \frac{d_i}{v_s}. \tag{7}$$

However, we wish to model two types of error: localization (global positioning system [GPS]) error and clock synchronization error. To model the GPS error, we add a vector, $\vec{u}$, sampled from a 2-D uniform distribution (from 0 to a user-specified d_{max}) to the microphone position before computing the distance to the known shooter position. This distribution implies that the latitude and longitude values have independent error. Alternatively, we could have chosen an offset direction from a uniform angle and magnitude, which would instead model a circular or Gaussian error joint distribution. In the error-free case, d_i was computed as

$$d_i = |0l_i - s|0. \tag{8}$$

With non-zero localization error, the distance to the known shooter is computed as

$$d_i^* = |0(l_i + \vec{u}) - s|0. \tag{9}$$

To add clock synchronization error to the model, we add a random value, t_{rand}, sampled from a uniform distribution from 0 to a user-specified t_{max} to the computed time it takes for the sound to reach the perturbed microphone position:

$$t_{ri}^* = t_{ri} + t_{rand} \tag{10}$$

3.2 User Interaction

3.2.1 Positioning the Microphones and the Shooter

The four microphone positions, as well as the shooter, which are added to the scene automatically, can be moved around by dragging the icons with the left mouse button. To add more microphones, simply choose Actors $\rightarrow$ Add Microphone from the menu, which will place a new microphone in a random position in the scene (which can be moved to the desired location). Microphones can be deleted from the scenario by holding control while right clicking on them.

The current number of microphones can be repositioned randomly by selecting Actors → Randomize Microphones from the menu. Similarly, the shooter position can be randomized by selecting Actors → Randomize Shooter Position.

3.2.2 Interacting with the Scene

The scene can be panned by holding down the mouse wheel and moving the mouse. The scene can be zoomed by either scrolling the mouse wheel or holding the right mouse button and moving the mouse.

3.2.3 Setting Error Parameters

By selecting View → Simulation Parameters from the menu, the user can display a dialog with sliders to set the clock-synchronization error variance and the GPS error variance.

3.3 Simulating a Gunshot

By selecting Simulate → GunShot from the menu, we compute the detected shooter position. (Of course, as the user has specified the position of the shooter, we have full knowledge of the scenario. We disregard this information in the computations after it has been used to generate the sound receipt times. However, it is exactly this information that allows us to determine the accuracy of our detected location.). In figure 6, we see the display after performing this action in an error-free case. The purple lines show the major axes of each of the four conics containing a subset of three of the microphones. (Note: The display of these lines, along with many other simulation elements, can be toggled by selecting View → Visualization Options.) We see that the shooter (gun symbol) has changed to a bullet, indicating the detected position. The detected position and detection error are displayed in the right-hand information bar.

Figure 7 shows the GUI after performing shooter detection in case with error. We see that the detected shooter position (bullet symbol) is not at exactly the same position as the known shooter (gun symbol). The detected position and detection error are displayed in the right-hand information bar. We also see slightly translucent sergeant logos near each original microphone position showing how the system interprets their GPS location including the introduced error.

3.4 Computing an Error Field

It is often interesting to see the quality of the detected shooter position (measured as a distance from the known shooter location) for a fixed microphone configuration across all possible shooter positions. We do this by moving the shooter to each integer-meter position on a grid across the

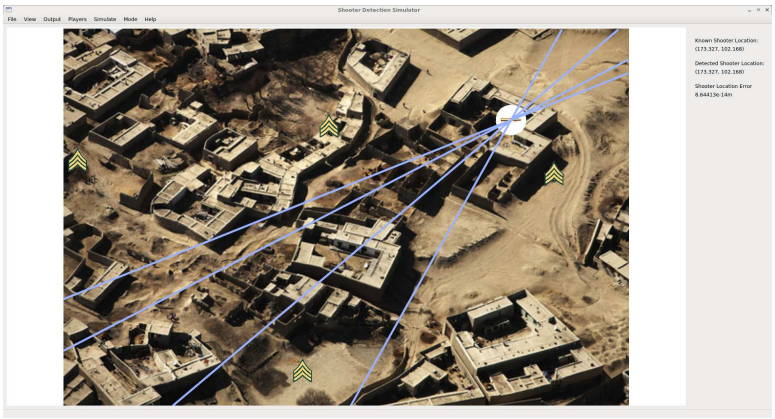

Figure 6. Our GUI after performing shooter detection in an error-free case. The purple lines show the major axes of each of the four conics containing a subset of three of the microphones. We see that the shooter (gun symbol) has changed to a bullet, indicating the detected position. The detected position and detection error are displayed in the right-hand information bar.

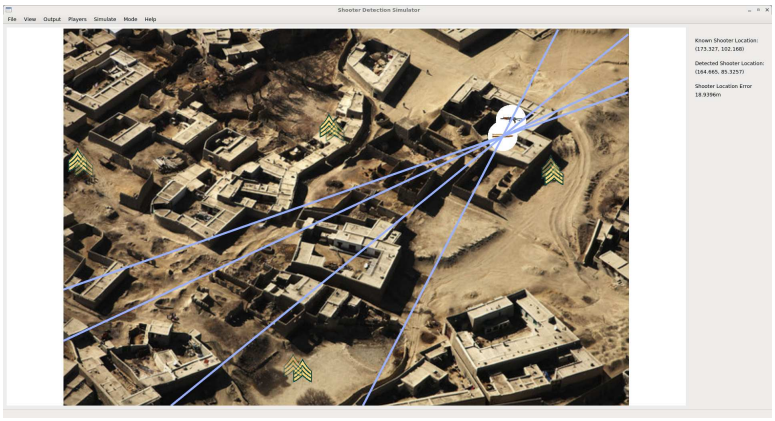

Figure 7. Our GUI after performing shooter detection in a case with error. We see that the detected shooter position (bullet symbol) is not at exactly the same position as the known shooter (gun symbol). The detected position and detection error are displayed in the right-hand information bar. We also see slightly translucent sergeant logos near each original microphone position showing how the system interprets their GPS location including the introduced error.

entire scene. This error field can be generated by selecting Simulate → Compute Error Field from the menu. Figure 8 shows an example error field. We pseudo-color the field and display a

color bar indicating the meaning of the color continuum. These error fields are used extensively in experiments in section 4.

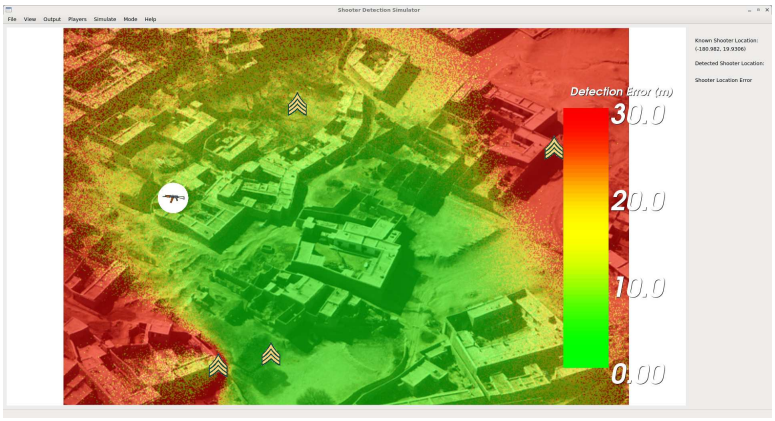

Figure 8. A visualization of the error-field showing the quality of the detection at all possible positions of a shooter relative to a static layout of microphones. As shown in the colorbar, green indicates excellent detections, while red indicates poor detections.

4. Error Analysis

As we have previously discussed, there are many factors that affect the quality of the detected shooter position. In this section, we present the results of several experiments that study the effects on the quality of the shooter detection produced by GPS localization error of each microphone, clock synchronization error between microphones, the geometry of the microphones, as well as the position of the shooter relative to the microphone configuration. Since there are some random values in the simulations, we have performed most experiments multiple times and taken medians and means where appropriate to present meaningful results.

4.1 System Error Analysis

4.1.1 Localization Error

In the ideal case, each microphone knows its location exactly. That is, the GPS coordinates computed on each device are perfectly accurate. However, it is well known that the GPS coordinates computed on a consumer-level handheld device are only accurate to about 10 m (in the best case—in future work, we will investigate this accuracy further) of the actual location. In

this experiment, we vary the localization error of all microphones and compute the corresponding detection error. In figure 9, we see that as the localization error increases, the resulting detection error also increases. We can also see that this behavior does not change as additional microphones are added to the simulation. We also see here the effect of the number of microphones. With four, we have the minimum required for the LOCA method to produce a solution, but the solution is quite sensitive to localization error. Adding a fifth microphone increases the number of triads from 4 to 10, greatly reducing sensitivity to error in any one of the point locations. Adding a sixth microphone provides 60 triads, but the extra information does not further reduce the sensitivity on the location accuracy.

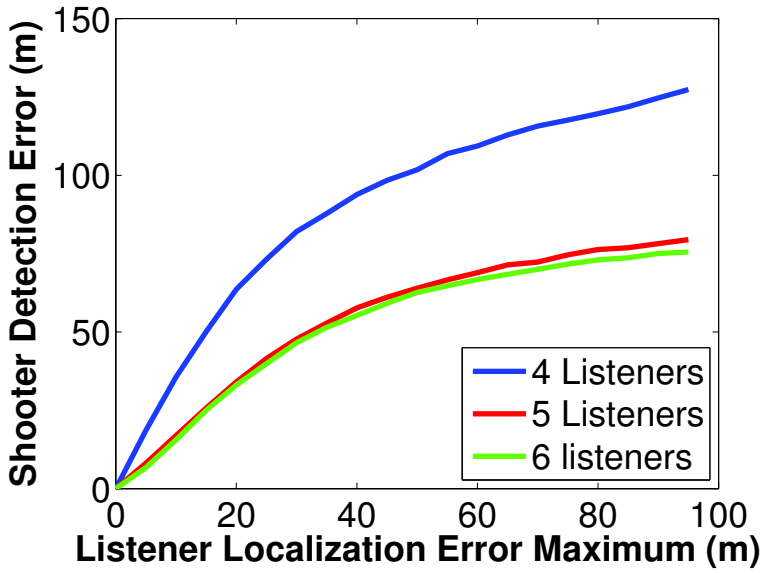

Figure 9. The median detection error of shooter positions varying over the entire scene over 1000 realizations of the simulation vs. uniform random localization errors of increasing magnitude.

4.1.2 Clock Synchronization Error

In the ideal case, the clocks of all microphones are synchronized exactly. That is, the time difference of arrival of the sound computed between two microphones (by subtracting the arrival time at each microphone according to each microphone's local clock) is exactly the amount of time that elapsed between the sound physically arriving at the microphones. However, maintaining clock synchronization is a difficult engineering challenge. In this experiment, we vary the clock synchronization error of all microphones and compute the corresponding shooter detection error. In figure 10, we show that increases in synchronization error lead to increases in shooter detection error.

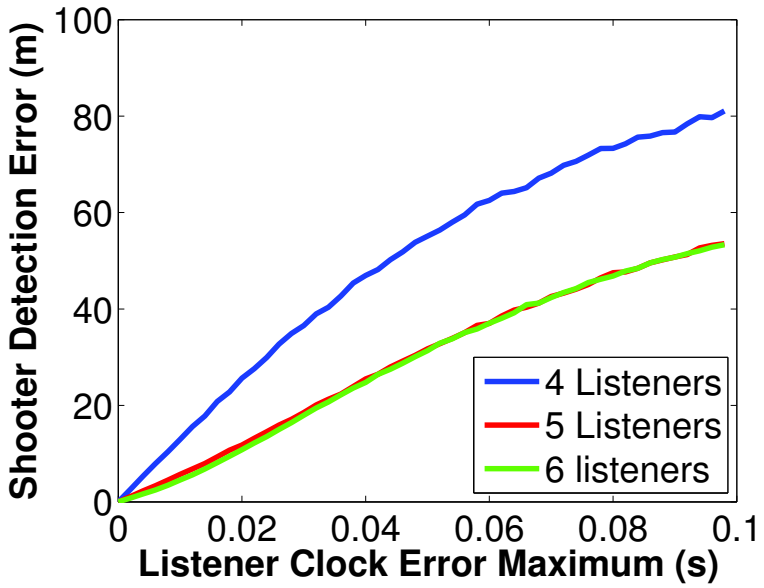

Figure 10. The median detection error over the entire scene over 1000 realizations of the simulation vs. uniform random synchronization errors of increasing magnitude.

We note that synchronization error can be interpreted as localization error in a perfectly synchronized system. The relationship is

$$\Delta d = v\Delta t \tag{11}$$

where v is the speed of sound in the conditions we have assumed for the experiment (343.2 m/s). This means that a 1-ms clock error corresponds to a 0.3432 m localization error. A comparison of the effects of these two sources of error is shown in figure 11. These curves are similar but not identical. This is because the localization error is measured as the distance from the actual microphone location to the perturbed microphone location, while the synchronization error assumes the displacement in location is along the line joining the shooter and the microphone.

4.2 Microphone Count/Configuration Error Analysis

4.2.1 Number of Microphones

This purpose of this experiment is to determine if the number of microphones, independent of their configuration, affects the quality of the shooter detection. For each fixed number of microphones (with bounds of 4 to 13 microphones, as at least 4 are required to obtain an unambiguous solution and at 13 we seem to reach an asymptote), we generate a set of random

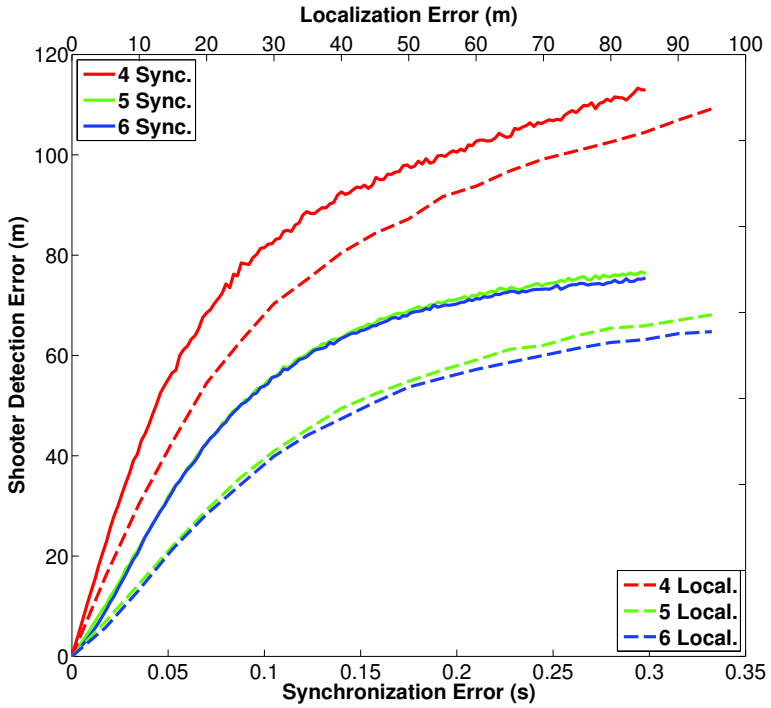

Figure 11. A comparison between the effects of clock synchronization and GPS localization error. The solid red, green, and blue curves show detection error (the median of 1000 experiments) due to synchronization error, while the dashed red, green, and blue curves show detection error due to localization error.

microphone positions and compute the median detection error over the set of all shooter positions in the scene. As shown in figure 12, the detection error decreases exponentially with the number of microphones.

4.2.2 Microphone Radius Error

In this experiment, we randomly choose microphone positions from a circle centered at the shooter. This represents an ideal configuration in which the microphones are likely to surround the shooter. This ideal configuration minimizes the redundancy of the information provided by each microphone, leading to the greatest possible accuracy given the localization errors. Three such radii are shown in figure 13. In figure 14, the shooter detection error is shown versus the radius of this circle for three microphone localization errors. We see that as the radius of the region that the microphone locations are selected from increases, the error in detected shooter location also increases. However, we notice that the detection error seems to asymptotically approach the specified microphone localization error.

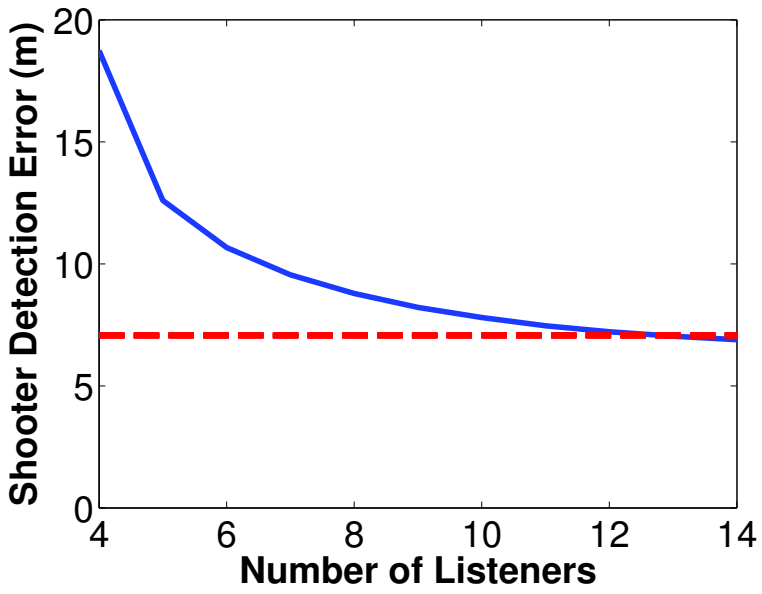

Figure 12. The median detection error of the shooter position varying over the set of all shooter positions in the scene using 100 sets of random microphone configurations for each fixed number of microphones. In each simulation, there is zero clock synchronization error and each receiver has a GPS localization error chosen from a uniform distribution from (–5 m, –5 m) to (5 m, 5 m). As a side effect of the latitude/longitude independence assumption, the distribution includes points that are up to $5\sqrt{2}$ from the actual location (half the diagonal of the square distribution). Therefore, the asymptote half the diagonal of the square distribution is at this value, indicated by the red dashed line.

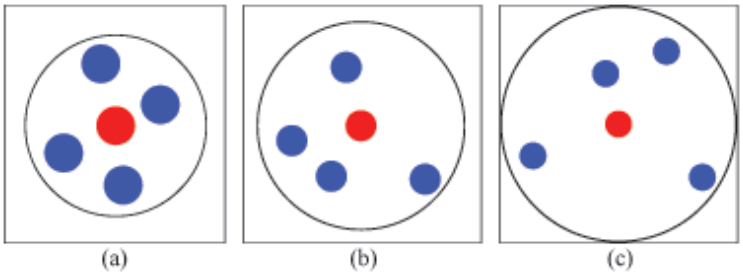

Figure 13. Three realizations of random microphone positions (blue) inside a varying radius around the shooter (red).

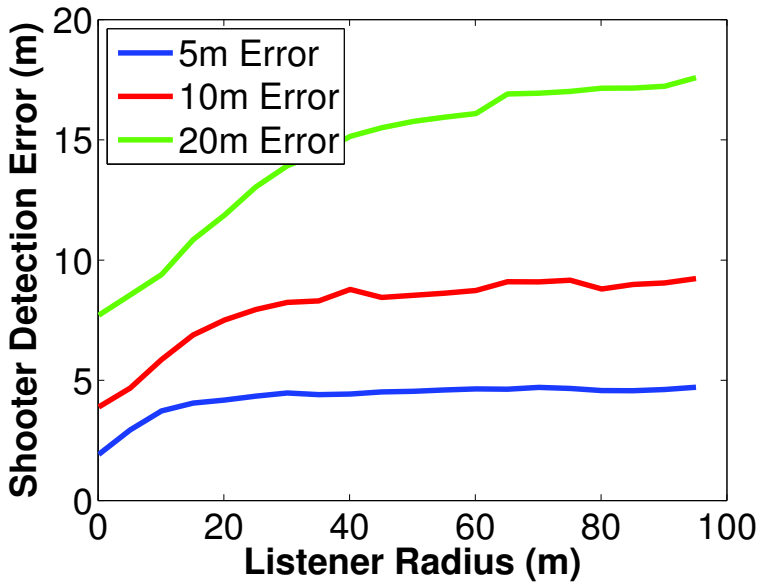

Figure 14. The median detection error over 1000 realizations of the simulation where five microphone positions are chosen randomly from a circle around the shooter with increasing radius.

4.2.3 Microphone Group Distance to Shooter Error

In this experiment, microphone positions are randomly selected from a circle of the same size, but the center of this circle is moved relative to the shooter position, as shown in figure 15. This represents a less than ideal configuration in which the information received by the microphones will be largely redundant, since the sound of the gunshot is coming from almost the same direction for all listeners. We expect that it should still be possible to accurately identify the direction of the gunshot, but not its distance. As the shooter-circle distance approaches infinity, the lines from the shooter to each mic become parallel. A small localization error could then lead to an enormous detection error, so we do not expect the error curve to level off asymptotically.

In figure 16, we see that the detection quality decreases as the distance from this circle to the shooter increases. The reason for this behavior is that we effectively lose ability to "triangulate" the shot in that the sound is only heard from one general direction by all microphones. We discuss in section 4.2.6 how this situation leads to major axes intersecting at very shallow angles, essentially amplifying any error.

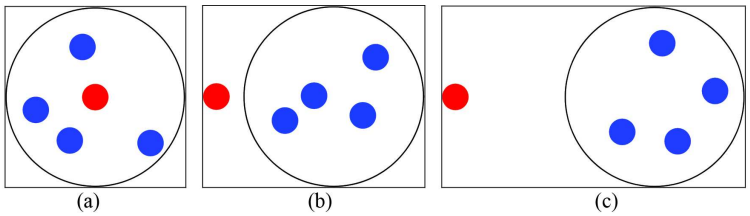

Figure 15. Three realizations of random microphone positions (blue) inside a fixed radius with varying distance to the shooter (red).

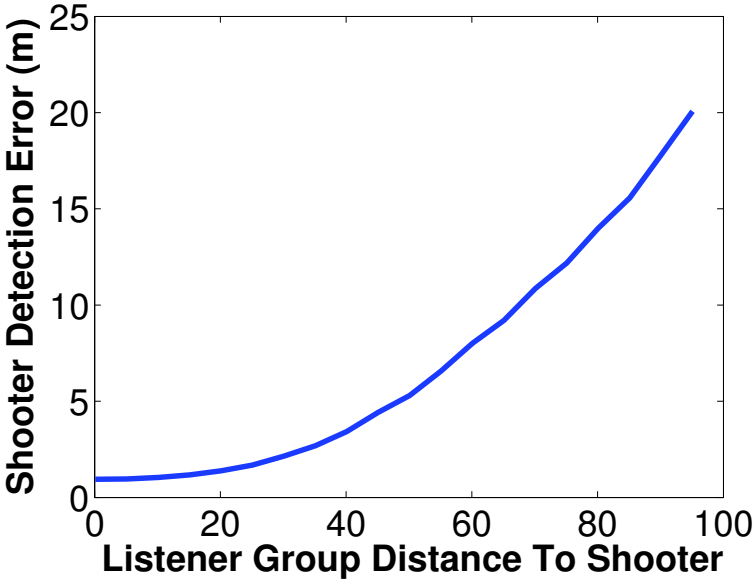

Figure 16. The median detection error over 1000 realizations of the microphone positions chosen randomly from a 50 m circle where the center of this circle is moved away from the shooter.

4.2.4 Microphone-Microphone/Shooter-Microphone Distance Ratio

In this experiment, we generate a random scene configuration. Then we compute the average distance between all pairs of microphones DM and the average distance between each microphone and the shooter DS and find their ratio $\frac{DM}{DS}$. The Microphone-Microphone/Shooter-Microphone Distance Ratio (MMSM ratio) is computed as

$$\frac{\frac{1}{|U_L|}\sum_{(i,j)\in U_L} D_{ij}}{\frac{1}{N_M}\sum_{i=1}^{N_M} D_i} \tag{12}$$

where N_M is the number of microphones, U_L is the set of unordered pairs of microphones (and $|U_L| = N_M(N_M - 1)/2$), D_i is the distance from the i^{th} microphone to the shooter, and D_{ij} is the distance between the microphones i and j. This metric is designed to capture the effects of the experiments Microphone Group Distance to Shooter Error and Microphone Radius Error simultaneously.

The intuition is that as the microphone arrangement is more compact and farther away from the shooter this ratio is low, and when the microphones are relatively spread apart but close to the shooter, this distance is high. Figure 17 shows an example scene where the MMSM ratio is low, while figure 18 shows an example scene where the MMSM ratio is high. In figure 19, we show that as this ratio increases (the microphones get farther away from each other with respect to their distance from the shooter), the detection error decreases. This curve captures several of the principles of good microphone placement, and we recommend it as a "rule of thumb" for determining the placement of microphones while planning a mission. Given an estimate of the average distance from the shooter to the microphones as well as a desired shot detection accuracy, we can read off this curve an appropriate distance between microphones. For example, if we know that the shooter is likely to be 100 m away from the microphones and we desire the detection error to be no worse than 10 m, we can see that the MMSM ratio should be about 1.1, and from $\frac{D_{MM}}{D_{SM}} = 1.1$ where $D_{SM} = 100$ we can compute D_{MM} to be 110 m.

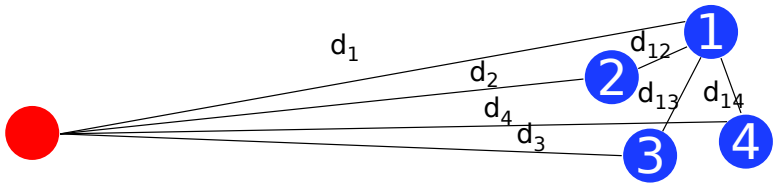

Figure 17. An example of a situation where the MMSM distance is low. Blue = microphone, Red = shooter. For clarity, the only microphone-microphone distances shown involve microphone 1.

4.2.5 Microphone Scene Coverage

In this experiment, we generate a random scene configuration. Then we compute the percentage of the scene that the convex hull of the microphones covers. In figure 20, we show examples of two microphone configurations, one with low coverage and the other with high coverage. Note that in both cases, not all microphones contribute to the convex hull. In figure 21, we show that as this ratio increases (the microphones cover more of the scene), the detection error decreases.

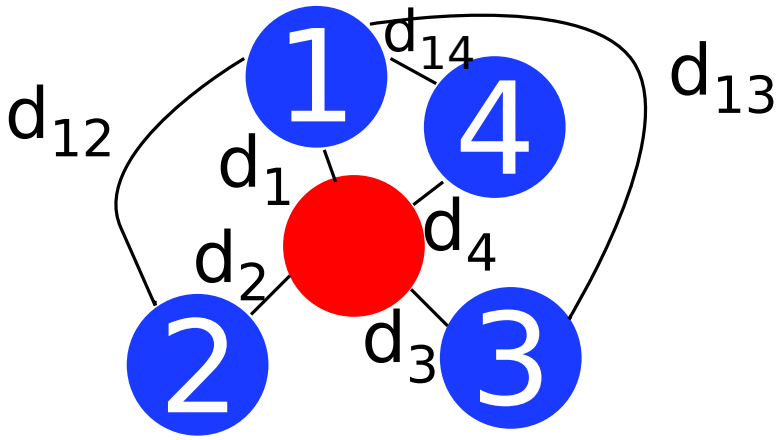

Figure 18. An example of a situation where the MMSM distance is high. Blue = microphone, Red = shooter. For clarity, the only microphone-microphone distances shown involve microphone 1.

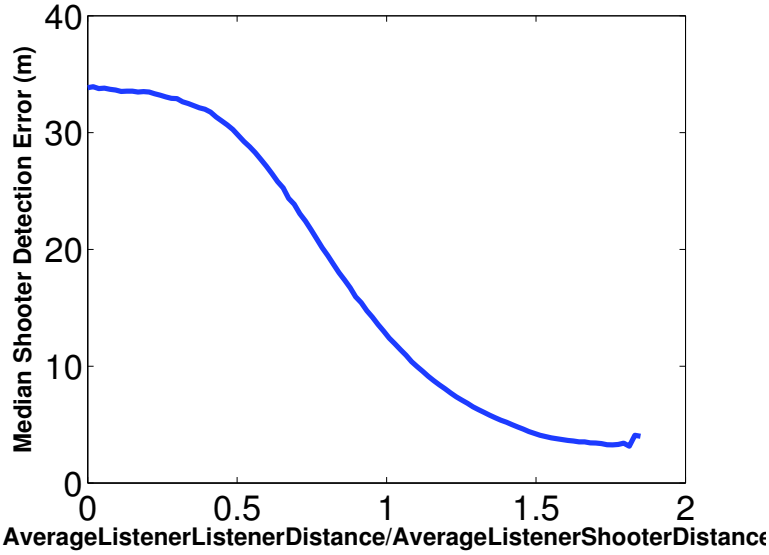

Figure 19. The median detection error over 1000 realizations of the microphone positions chosen randomly from a 50-m circle where the ratio of the average microphone-microphone distance to the average microphone-shooter distance is varied. The detections are higher accuracy when this ratio is high.

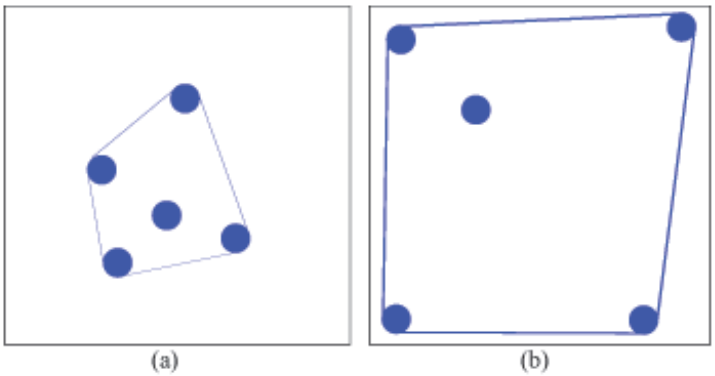

Figure 20. (a) An example scene with a low coverage ratio.
(b) An example scene with a high coverage ratio.

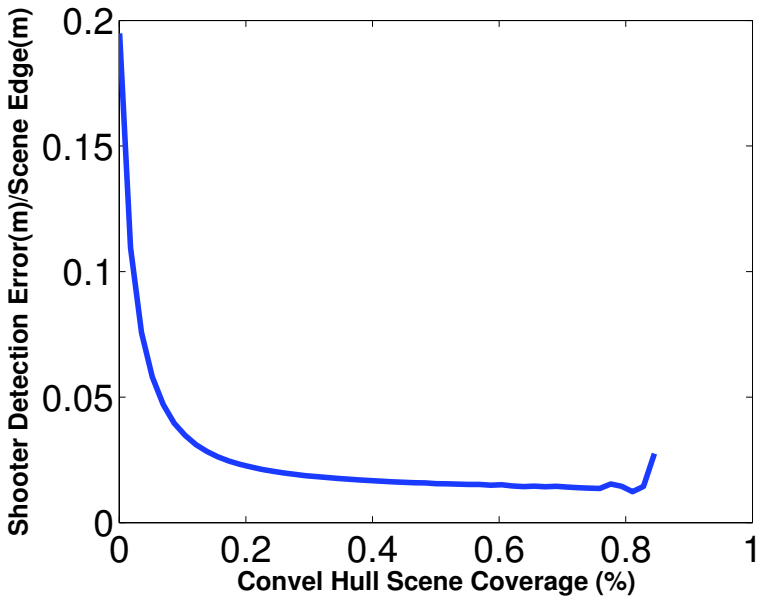

Figure 21. The convex hull coverage percentage vs. the median detection error over 1,000,000 realizations of the microphone positions chosen randomly over the scene. The error is reported as a ratio of the actual detection error and the size of the scene (in this case, the scene is 200 m x 200 m).

4.2.6 Angle Between Major Axes

The LOCA method identifies the intersection between two lines (the major axes). We can compute the angle θ between two major axes $A_1x + B_1y + C_1 = 0$ and $A_2x + B_2y + C_2 = 0$ as

$$\theta = atan\left(\frac{A_2B_1 - A_1B_2}{A_1A_2 + B_1B_2}\right). \tag{13}$$

This expression allows us to directly see the effect of changing the location of a microphone on the angle between the major axes of the resulting configuration. The angle between the major axes of the conics produced by each subset of three microphones is a strong indicator of the stability of the shooter detection solution. Consider one of the major axis lines as a reference coordinate system. The intersection of the two lines is moved along the reference line exactly the amount of the localization error parallel to the reference line. However, the intersection point of the two lines is also moved along the reference line because of localization error perpendicular to the reference axis by an amount proportional to the angle α between the lines.

A diagram of the situation is shown in figure 22. Using Major Axis 1 as the reference axis, Δx is the localization error along Major Axis 1, and Δy is the localization error orthogonal to Major Axis 1. The constant of proportionality can be derived via a similar triangles argument. From the definition of the tangent, we have

$$\tan(\alpha) = \frac{y^*}{x^*} = \frac{y + \Delta y}{x + \Delta x}. \tag{14}$$

If we consider the case where $x \to 0$ and $y \to 0$, we see that

$$\tan(\alpha) = \frac{\Delta y}{\Delta x}. \tag{15}$$

The localization error orthogonal to the reference axis therefore produces an intersection/detection error of

$$\text{Detection Error} = \frac{1}{\tan(\alpha)}\Delta y. \tag{16}$$

To show that this is indeed the behavior of the detection error, we ran $10,000$ simulations and recorded the average angle between all pairs of the four major axis lines in the LOCA solution and the corresponding shooter detection error. A plot of this error is shown in figure 23.

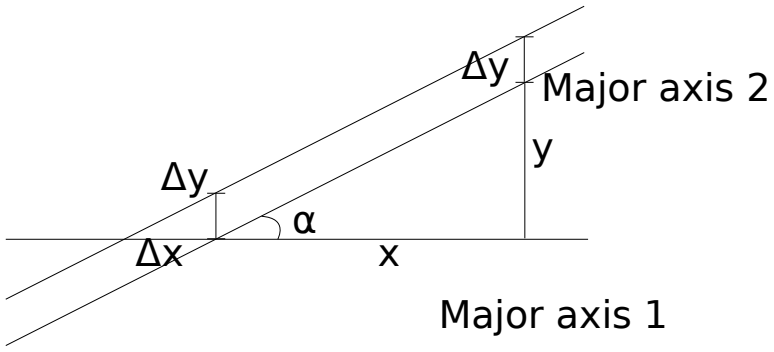

Figure 22. The geometry of the detection error introduced by localization error.

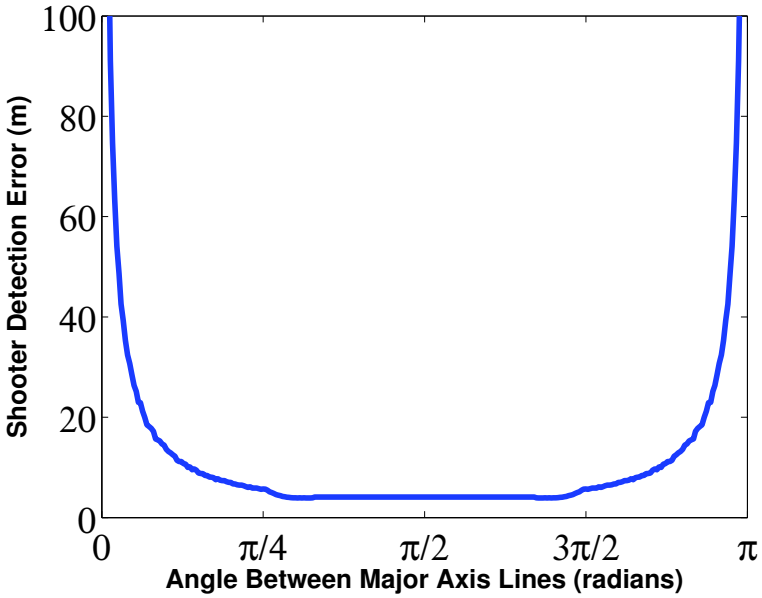

Figure 23. The error in intersection versus the orthogonal error in localization. We see that when the major axes are orthogonal (at $\frac{\pi}{2}$), the best detection accuracy is obtained, and when they are parallel (at 0 and π), the detection error is very high.

4.3 Probability of Quality Detection

With a particular microphone geometry, gunshots in some regions of the scene can be detected well, while in other regions we expect high detection error. To show this effect, we have placed the shooter at every position in the scene, and at each position performed several simulations. We computed the average detection error over the simulations at each position, and used those values

to color code an overlay, which can be interpreted as describing the expected quality of detection in regions over the scene.

4.3.1 Four Microphones

In this section, we again make the case for using more than the minimum (four) number of microphones. In figure 24, we show a "good" configuration of four microphones. Green pixels describe regions from which if a shot was fired, we would trust the computed location. On the other hand, red regions show positions in which if a shooter was present, we would not compute an accurate location. Since the listeners are spread over a large percentage of the scene, detection errors are low in most regions, as predicted by the results in section 4.2.5. We see that even in this ideal spacing and coverage configuration, there are still large regions of poor detection quality.

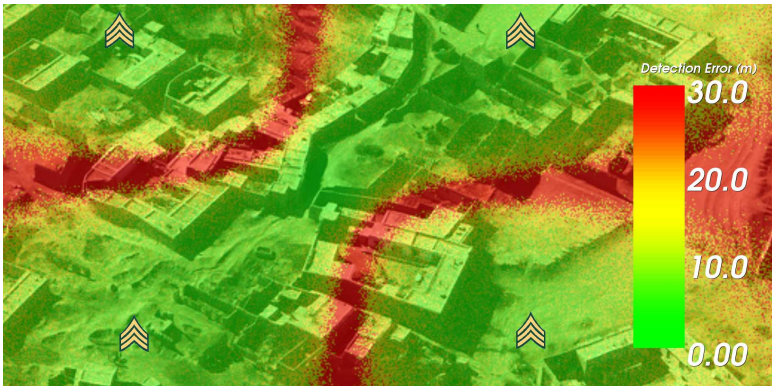

Figure 24. A pseudo-colored scene indicating regions of expected high quality detections (green) and low quality detections (red). Four microphones spread out provides good overall coverage, but still leaves gaps.

In figure 25, we show a configuration of four microphones arranged in a small square. Again as predicted by section 4.2.5, since the percentage of the scene covered by the convex hull is low, the expected shooter detection error is high.

In figure 26, we show four microphones arranged in a nearly linear configuration. We see that this configuration yields particularly poor detection quality. Not only is the percentage of the scene covered by the convex hull low, but so is the angle between the major axes in the regions to the left and right of the listeners. The only regions that would result in accurate shooter detections are therefore close to the group of listeners and either above or below.

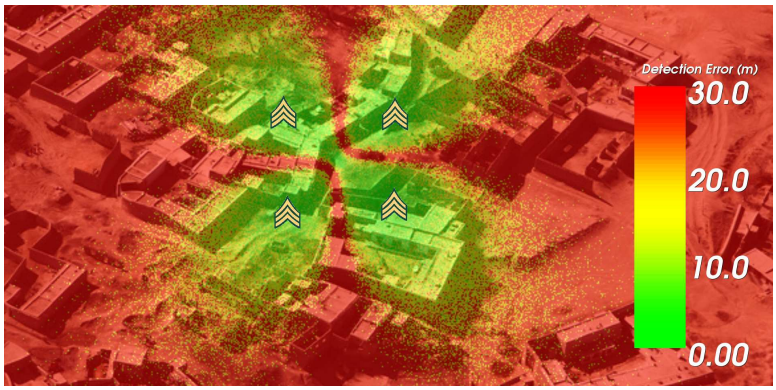

Figure 25. A pseudo-colored scene indicating regions of expected high quality detections (green) and low quality detections (red). Drawing the four microphones closer together leaves more of the scene uncovered.

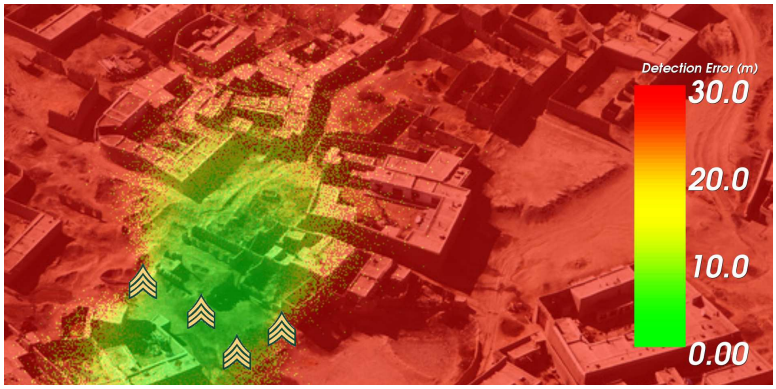

Figure 26. A pseudo-colored scene indicating regions of expected high quality detections (green) and low quality detections (red). Placing the microphones in a relatively linear configuration only provides coverage perpendicular to that line.

4.3.2 Five Microphones

In figure 27, we show that with five microphones in a good configuration, we get much better coverage over the whole map (as we saw in figures 9–12).

In figure 28, we see that no matter how many microphones are available, if they are all in the same location, the detections will be poor no matter where the shooter is located. Microphones that are close to each other provide redundant information, so they do not help to reduce detection error.

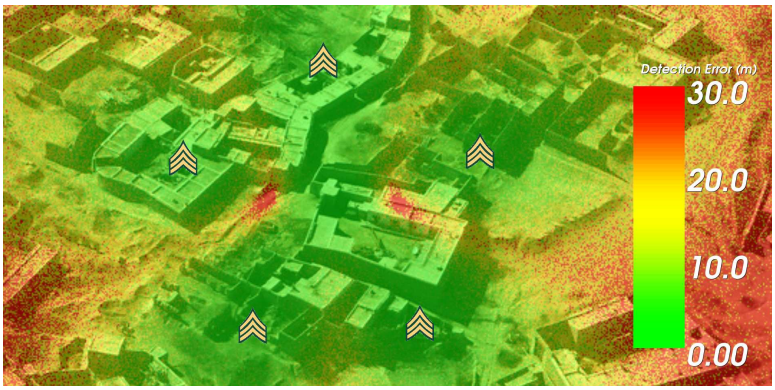

Figure 27. A pseudo-colored scene indicating regions of expected high quality detections (green) and low quality detections (red). Adding a fifth microphone covers most of the gaps that were left uncovered by just four microphones.

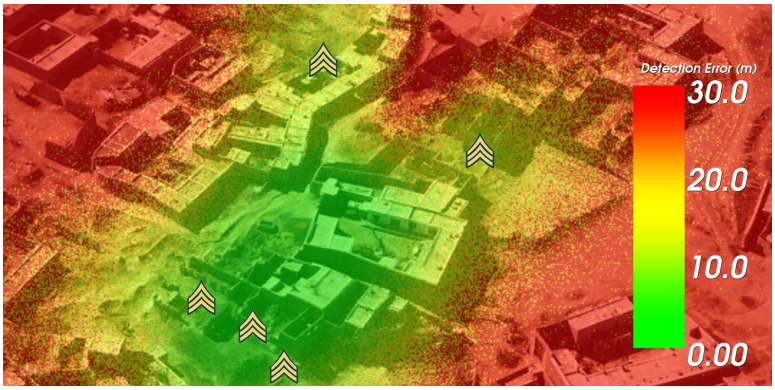

Figure 28. A pseudo-colored scene indicating regions of expected high quality detections (green) and low quality detections (red). The three microphones that are located near each other provide redundant information, doing little to reduce detection error.

In figure 29, we show an arrangement of five microphones in a non-ideal, but not degenerate configuration. As in figure 27, the relatively close and linear configuration of listeners only provides coverage that is nearby and perpendicular.

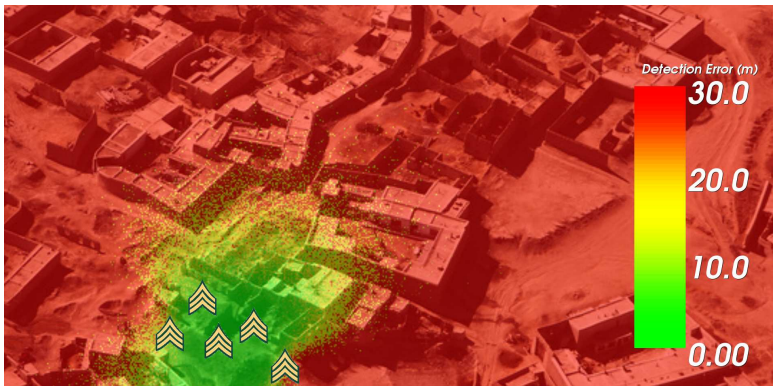

Figure 29. A pseudo-colored scene indicating regions of expected high quality detections (green) and low quality detections (red). Placing the listeners in a relatively linear configuration only provides coverage perpendicular to that line. Adding additional listeners nearby and in the same line does not increase coverage.

5. Conclusions

In this report, we have described the design of a software simulator for studying various behaviors of a shooter detection algorithm. We have detailed the response of the simulator to parameters such as GPS error, clock synchronization error, the number of microphones, and microphone configuration. Our main purpose was to show that this type of offline analysis can be beneficial to understanding the specifics of when and why shooter detection works well, as well as when it does not. We have shown that the number and configuration of microphones is an important consideration when deploying such a system, and that at least five microphones are required to obtain reasonable detections. We have noted that it is highly desirable for the convex hull of the microphones to enclose the shooter's position. Finally, we have shown that the region of high accuracy detection is not typically intuitive, often quite complex, and certainly worth considering while designing systems and planning missions. We conclude this report with a bulleted summary of ideas that are important to consider when designing a shooter detection system or planning a mission to use such a system.

5.1 Recommendations and Lessons Learned

- At least five microphones should be used for the highest accuracy detections.

- Placing all microphones close together will only produce accurate detection in a small region.
- Placing microphones in a line only provides accurate detections perpendicular to that line.
- Based on the expected threat distance and observed GPS localization and synchronization errors, it is possible to calibrate figure 19 in order to provide a "rule of thumb" distance between microphones for high accuracy shooter detection while planning a mission.

6. Future Work

Theoretically, one could derive an analytical expression of the detection error as a function of the microphone locations, the localization errors, and the synchronization errors. This would allow queries of these estimated detection accuracy values as simple function evaluations rather than complex simulations, which could make it possible to provide Warfighters with real-time estimates of shooter detection quality within their vicinity, like those shown in figures 24–29. Furthermore, it would allow us to optimize parameters of the scenario directly to answer questions such as "Where should I place the microphones to maximize the area of high accuracy detection?" This optimization problem could even include constraints such as restricted areas of the microphones, the maximum distance between microphones, etc.

7. References

1. Raytheon Boomerang Shooter Detection System. *http://bbn.com/products_and_services/boomerang/boomerang_warrior_x* (accessed September 2013).

2. QinetiQ EARS Gunfire Detection System. *http://www.qinetiq-na.com/products/survivability/ears/* (accessed September 2013).

3. Sallai, J.; Volgyesi, P.; Ledeczi, A.; Pence, K.; Bapty, T.; Neema, S.; Davis, J. Acoustic Shockwave-Based Bearing Estimation. *Information Processing in Sensor Networks* **2013**.

4. Doria, David. *A Detailed Solution to the Hyperbolic Lines Of Position Formulation of the Shooter Detection Problem*; ARL-TR-6592; U.S. Army Research Laboratory: Adelphi, MD, 2013.

5. Schmidt, Ralph. A New Approach to Geometry of Range Difference Location. *IEEE Transactions on Aerospace and Electronic Systems* **1972**, *8*.

6. Klukas, R. W. Acoustic Shockwave-Based Bearing Estimation. A Superresolution Based Cellular Positioning System Using GPS Time Synchronization, 1997.

Appendix. Any Two Triads of Microphones Produce the Same LOCA Solution

We show symbolically (using Mathematica 8.0.4.0) that the linear system consisting of any three (out of four) of the major axis lines generated in the LOCA procedure intersect at exactly the same point. We do this by showing that the determinant of the matrix of system coefficients can be simplified to zero, indicating that the equations are linearly dependent.

Microphones 1,2,3

$$A1 = x1 * D23 + x2 * D31 + x3 * D12;$$

$$B1 = y1 * D23 + y2 * D31 + y3 * D12;$$

$$C1 = -.5*(D12*D23*D31+(x1\text{^}2+y1\text{^}2)*D23+(x2\text{^}2+y2\text{^}2)*D31+(x3\text{^}2+y3\text{^}2)*D12);$$

Microphones 1,2,4

$$A2 = x1 * D24 + x2 * D41 + x4 * D12;$$

$$B2 = y1 * D24 + y2 * D41 + y4 * D12;$$

$$C2 = -.5*(D12*D24*D41+(x1\text{^}2+y1\text{^}2)*D24+(x2\text{^}2+y2\text{^}2)*D41+(x4\text{^}2+y4\text{^}2)*D12);$$

Microphones 2,3,4

$$A3 = x2 * D34 + x3 * D42 + x4 * D23;$$

$$B3 = y2 * D34 + y3 * D42 + y4 * D23;$$

C3 = $-.5*$(D23$*$D34$*$D42$+$(x2^2$+$y2^2)$*$D34$+$(x3^2$+$y3^2)$*$D42$+$(x4^2$+$y4^2)$*$D23);

Linear System/Determinant

$$m = \begin{pmatrix} A1 & B1 & C1 \\ A2 & B2 & C2 \\ A3 & B3 & C3 \end{pmatrix};$$

determinant = Det$[m]$;

Substitutions

These substitutions are from the definition of the distance differences, as well as the fact that the distance difference between i and j is the negative of the distance difference between j and i.

D12 = D2 $-$ D1;

D13 = D3 $-$ D1;

D14 = D4 $-$ D1;

D23 = D3 $-$ D2;

D24 = D4 $-$ D2;

D34 = D4 $-$ D3;

D21 = $-$D12;

D31 = $-$D13;

$D32 = -D23;$

$D41 = -D14;$

$D42 = -D24;$

Symbolic Simplification

FullSimplify[determinant]

0.

INTENTIONALLY LEFT BLANK.

NO. OF COPIES	ORGANIZATION
1 (PDF)	DEFENSE TECHNICAL INFORMATION CTR DTIC OCA
2 (PDF)	DIRECTOR US ARMY RESEARCH LAB RDRL CIO LL IMAL HRA MAIL & RECORDS MGMT
1 (PDF)	GOVT PRINTG OFC A MALHOTRA
6 (PDF)	DIRECTOR US ARMY RESEARCH LAB RDRL CIH S D DORIA P SCHWARTZ D SHIRES D BRUNO R TAYLOR S PARK

INTENTIONALLY LEFT BLANK.